Structures 56 (2023) 104920

Contents lists available at ScienceDirect

Structures

journal homepage: www.elsevier.com/locate/structures

# Comparative performance analysis of ground slabs and beams reinforced with macro polypropylene fibre, steel fibre, and steel mesh

Feng Shi [a], Thong M. Pham [b,*], Rabin Tuladhar [c], Zongcai Deng [d], Shi Yin [a], Hong Hao [e,f,*]

[a] Ningbo Shike New Material Technology Co. Ltd, Ningbo, China
[b] UniSA STEM, University of South Australia, Mawson Lakes, SA, 5095, Australia
[c] College of Science & Engineering, James Cook University, QLD 4811, Australia
[d] The Key Laboratory of Urban Security and Disaster Engineering, Ministry of Education, Beijing University of Technology, Beijing 100124, China
[e] Guangdong Provincial Key Laboratory of Earthquake Engineering and Applied Technology, Earthquake Engineering Research and Test Center, Guangzhou University, China
[f] Center for Infrastructural Monitoring and Protection, School of Civil and Mechanical Engineering, Curtin University, Kent Street, Bentley, WA 6102, Australia

ARTICLE INFO

*Keywords:*
Fibre reinforced concrete
Slabs
Steel fibres
Polypropylene fibres
Beams

ABSTRACT

This study examines the structural performance of concrete slabs and beams reinforced with various types of reinforcement under centrally concentrated loading until failure. Three types of reinforcement were studied, including steel meshes (A142), steel fibers (30 kg/m$^3$), and macro polypropylene (PP) fibers (6 kg/m$^3$). The study discusses the fracture behavior of ground slabs and the enhancement in performance resulting from the inclusion of PP and steel fibers in terms of load–strain and load–deflection responses, deflection profiles, and crack patterns. In addition, the study compared the flexural behavior of fiber-reinforced concrete beams to determine the effectiveness of using various fibers in beams and slabs. The results revealed a significant increase in the flexural strength of steel fiber or steel mesh reinforced slabs on the ground as compared to the reference specimen while slabs reinforced with PP fibers showed favorable results in post-cracking performance and energy absorption compared to steel fibers. The use of PP fibers, steel fibers, and steel meshes can improve the flexural cracking strength of concrete slabs by 28%, 47%, and 79%, respectively. However, predictions based on the beam tests and physical properties of steel mesh overestimated the flexural strength of ground slabs by 12%, while the corresponding predictions of PP fiber-reinforced slabs and steel fiber-reinforced slabs were 45% and 24% higher than the experimental results. This study provides insights into the performance of different types of reinforcements in concrete slabs and beams, which can be valuable in designing and constructing reinforced concrete structures.

## 1. Introduction

Concrete ground slabs are widely used in a range of applications, including industrial slabs, footpaths, highways, and decorative floorboards. Industrial concrete slabs must be capable of supporting heavy loads resulting from operational movements of vehicles and stored materials [1,2]. In recent years, an innovative solution for the repair, rehabilitation, and reconstruction of pavements, known as Precast Concrete Pavement Systems, has been developed and it offers many advantages, including a long life expectancy, low maintenance costs, and quick placement, thereby reducing traffic congestion [3]. Decorative concrete floorboards are also becoming increasingly popular in modern buildings due to their surface patterns, skid resistance, and fire safety, which are comparable to those of natural granite thin slabs [4]. However, the design and construction of reinforced concrete slabs and pavement systems require an understanding of the performance of different types of reinforcements.

The performance of ground slabs, whether in residential, industrial, or commercial buildings, is influenced by various factors, including the compressive and tensile strengths of concrete, as well as the properties of ground [5]. To achieve crack-free slab surfaces, it is essential to ensure that the slabs possess sufficient load capacity and effective control of cracking and crack widths. This is typically achieved through the use of reinforcement bars or welded meshes to reinforce the concrete slabs. By incorporating these reinforcements, the tensile strength of the concrete can be enhanced, allowing for increased load-carrying capacity and

* Corresponding authors.
*E-mail addresses:* thong.pham@unisa.edu.au (T.M. Pham), hong.hao@curtin.edu.au (H. Hao).

https://doi.org/10.1016/j.istruc.2023.104920
Received 7 March 2023; Received in revised form 16 July 2023; Accepted 17 July 2023
Available online 21 July 2023

improved control over crack formation and propagation. In this way, the use of reinforcement can significantly improve the performance of ground slabs, enabling them to withstand the demands of heavy loads and ensuring their longevity in a range of applications.

However, the use of steel bars and meshes is not only time-consuming and labour-intensive but also sometimes not suitable for ultra-thin slabs or mechanised production. Steel bars and meshes also cannot control surface cracking well because they need to be placed a distance away from the surface. In recent years fibre-reinforced concrete (FRC) ground slabs have obtained considerable momentum. Steel fibres and macro polypropylene (PP) fibres are increasingly used to replace steel meshes in concrete slabs [6,7] and other structures [8,9]. Steel fibres can not only effectively improve the compressive and tensile strengths of concrete, but also prevent concrete cracking and improve the toughness and post-cracking performance of concrete [10]. Since steel fibres are vulnerable to rusting and may cause cuts and bruises to the construction workers and users, macro PP fibres are increasingly becoming popular to reinforce concrete slabs. Macro PP fibres can efficiently control cracking and improve the toughness and post-cracking performance of concrete [11,12]. Moreover, macro PP fibres are easy to disperse in concrete, safe to handle, and corrosion resistant [13,14].

The majority of previous studies on the performance of fibre-reinforced concrete have focused on the flexural tests on concrete beams, which are used in design analysis of ground slabs [15–18]. However, the behaviour of flexural tests on beams may not truly represent the response of ground slabs. Only a few studies on fibre-reinforced concrete ground slabs have been reported so far [5]. Meanwhile, it is insufficient to use the results of the flexural tests to predict the performance of concrete ground slabs. This lack of results and understanding highlights the need of more studies on fibre-reinforced concrete ground slabs.

Jan Øverli [19] conducted an experimental and numerical investigation of a ground slab subjected to concentrated loading at the centre, the edges, and the corners. The main goal was to study the formation of cracks on the top surface which is often of concern in this type of structure. The slab had a square geometry with dimensions 3500 × 3500 × 120 mm. The nonlinear behaviour of the slab was captured by performing nonlinear finite element analyses. The results indicated that drying shrinkage could cause severe cracking in slabs on the ground. Amir [5,20] studied the mechanical and physical performance of steel and macro PP fibre-reinforced concrete ground slabs at an industrial scale. The loadings were carried out at different locations (centre, edges and corners) of a 6 × 6 × 0.15 m fibre-reinforced concrete slab. The results showed that the applied loads at the punching shear failure of macro PP fibre-reinforced concrete slabs were comparable to those reported for the steel fibre-reinforced concrete slabs under similar conditions. Roesler et al., [21,22] completed concentric loading tests on plain, steel fibre and macro PP fibre-reinforced concrete ground slabs. The slab dimensions were 2.2 × 2.2 m with a nominal thickness of 127 mm. The shape of the load–deflection curves indicated that the PP and the steel fibre-reinforced concrete slabs behaved similarly at different stages of cracking. Although PP fibres only slightly improved the tensile cracking load compared with the plain concrete slab, the flexural cracking load of the PP fibre slab (with the fibre ratio of 0.32% and 0.48% by volume) increased by 25% and 32% with respect to the reference specimen under the center loading, respectively. It should be noted that the previous studies only compared the performance of plain concrete and FRC slabs while there is no direct and comprehensive comparison between plain concrete ground slabs and those with steel meshes.

This study carries out an experimental investigation on the structural performance of concrete ground slabs with various types of reinforcements. The performance of plain ground slab and slabs reinforced with steel meshes, steel fibres and macro PP fibres subjected to concentrated loading was examined. The fracture behaviour and the contribution of fibres to the performance of concrete slabs on ground were discussed. In addition, the flexural behaviour of concrete beams with the same concrete mixes used for the slabs were tested and compared to the ground slabs to examine the different effects of using fibres in beams and slabs. The test results demonstrated that the performance of FRC ground slabs is different from that of FRC beams, therefore the design analysis based on outcomes from FRC beams might not give good results of ground slabs.

## 2. Methodology and procedures

### 2.1. Fibre, steel mesh and concrete mix

In this study, PP fibres, steel fibres and steel meshes were used to reinforce the concrete slabs as shown in Fig. 1. The properties of fibres and steel meshes are provided in Table 1. For A142 steel meshes, a diameter of 6 mm and distance between the main wire and cross wire of 150 mm was used in this study. In order to maintain an appropriate concrete cover, 30 mm wood bar chairs were used under the steel to raise it slightly off the bottom. Based on industry practice, a standard mix design for 40 MPa concrete was used in this study (as summarised in Table 2). This design is commonly used to construct concrete pavements. Fibres were added into the concrete batch plant and mixed with concrete. The fibre-reinforced concrete was delivered by a standard concrete truck. The average slump was 100 mm based on AS 1012.3.1–2014 [23]. Four slabs with the dimension of 1800 × 1800 × 120 mm were cast and vibrated by a vibration rod. As per AS 1012.8.1:2014 [24], concrete slabs, beams and cubes were removed from moulds after 24 h. All the specimens were then cured in a standard moisture room for 28 days. The processes are shown in Fig. 2.

### 2.2. Slab testing configuration

#### 2.2.1. Subgrade conditions of testing facility

This study aims to investigate the flexural performance of fibre-reinforced concrete ground slabs. As mentioned in the previous studies by Alani and Beckett [5], if the ground conditions are too stiff, it is hard to attain adequate bending of the slab. Therefore, sand was filled into a sand containment box of 2.1 × 2.1 × 0.4 m (as shown in Fig. 3) as the subgrade. Before each test, the sand was loosened and compacted into a low-plasticity condition. The modulus of subgrade reaction (κ) of near-to-surface properties of the subgrade was tested by the plate bear test to make sure that each plate settlement had the same level of sand compaction. The κ of sand was kept at about 0.05 N/mm$^3$.

#### 2.2.2. Slab test setup

Loading was applied at the centre of 1800 × 1800 mm slabs with a nominal thickness of 120 mm placed on the sand in the sand box. The tests were performed by using a 1000 kN hydraulic actuator. Under the hydraulic actuator, there was a load cell recording the applied load. The load was applied to the slab through a steel plate (100 × 100 × 10 mm) and a rubber plate (100 × 100 × 5 mm) to counteract any uneven surface on the slabs, as shown in Fig. 4. The load was applied with displacement control and the loading rate was 0.3 mm/min. In total, 20 linear variable differential transformers (LVDTs) and 8 strain gauges were placed at the top and bottom of each slab, as shown in Fig. 5.

#### 2.2.3. Instrumentation and data acquisition system

The deflections of slabs, internal bending strain, and the applied load were measured during the testing until failure. Deflections of the slabs in different locations were monitored using totally 20 LVDTs at various locations across the slab surface as shown in Fig. 5.

The tensile and compressive strain of the concrete slabs was recorded by 8 strain gauges (SGs) and their locations are shown in Fig. 5. The compressive strain (SG 5 and 7 in cross directions) and tensile strain (SG 6 and 8 in cross directions) were measured by the strain gauges installed at the top and bottom of the slab next to the load plate, respectively. SGs 1 to 4 were used to monitor strain on the top of the slab once the initial

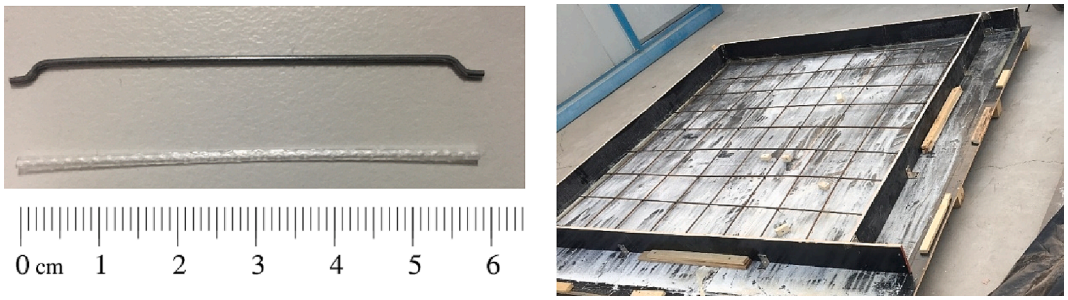


**Fig. 1.** Macro PP fibres, steel fibres and steel mesh.

**Table 1**
Properties of fibres and steel mesh.

| Properties | Macro PP fibre (PP fibre) | Steel fibre | Steel mesh |
|---|---|---|---|
| Diameter (mm) | 0.6 | 0.3 | 6 |
| Length (mm) | 50 | 50 | – |
| Length-to-diameter ratio | 83 | 167 | – |
| Tensile strength (MPa) | 650 | 1500 | 300 (yield stress)- |
| Elastic modulus (GPa) | 10 | 210 | 195 |
| Surface and shape | Indented surface | Hooked-end | Deformed bar |
| Dosage (volume percentage) | 6 kg/m$^3$ (0.7%) | 30 kg/m$^3$ (0.4%) | One layer at bottom |

**Table 2**
Concrete mix proportion.

| 40 MPa Concrete | Material (kg/m$^3$) |
|---|---|
| Cement | 186 |
| Fly ash | 134 |
| 0.075–0.3 mm Fine sand | 350 |
| 0.6–4.75 mm Fine aggregates | 610 |
| 6.7–9.5 mm Coarse aggregates | 260 |
| 9.5–19 mm Coarse aggregates | 690 |
| superplasticizer | 2.8 |
| Air entrapment admixture (ml/ 100 kg cementitious materials) | 22 |
| Water | 116 |

flexural cracking occurred on the top surface of the slab. These strain gauges were used to discuss and derive the point of crack initiation.

The comprehensive flexural performance of the slabs is discussed with respect to several parameters, including the visual crack observations, abrupt reductions of the applied load, and significant changes in the load–strain data. The tensile cracking load is defined when strain gauges begin displaying nonlinear behaviour [22]. The flexural cracking load is defined at the turning point in load–deflection curve, a considerable change in internal strain distribution, and visual cracking on the slabs [21]. The ultimate load-carrying capacity is defined as the collapse load, which was either a punching shear failure or a circumferential crack on top of the slab near the load plate.

### 2.3. Fibre-reinforced concrete material tests

#### 2.3.1. Compression tests

Compression tests were performed on the fibre-reinforced concrete specimens according to GB/T 50081-2002B [25]. Fibre-reinforced concrete cubes of 100 × 100 × 100 mm were tested at an age of 28 days. The tests involved the axial loading of a cube specimen until failure in the universal testing machine with a maximum load capacity of 2000 kN. The compressive strength of concrete with each fibre type was based on an average value of four identical specimens.

#### 2.3.2. Residual flexural strength with CMOD

Post-cracking behaviour of fibre-reinforced concrete beams was studied using a residual flexural strength test with crack mouth opening displacement (CMOD), according to BS EN 14651–2005 + A1-2007 [26]. The flexural beams had a size of 150 × 150 × 600 mm. A notch of 2 mm width and 25 mm depth was cut at mid-span of each beam. The notched beams were loaded using a 500 kN hydraulic testing machine on a three-point loading setup. The CMOD was measured using two clip gauges installed at the centre of the notch and averaged CMOD values were derived. The clip gauges attached to knife edges, which were glued to the bottom of the beam, were connected to a computerised data acquisition system and an LVDT, as shown in Fig. 6. The tests were displacement-controlled to achieve a constant rate of CMOD at 0.05 mm/min. Three identical samples for each fibre type were tested. Two plain concrete beams were tested as the control specimens.

#### 2.3.3. Flexural performance of beams with four-point loading

The flexural performance of fibre-reinforced concrete beams was studied using flexural tests with four-point loading on the unnotched beams, according to ASTM C1609 [26]. The tested beams had a square cross-section of 150 × 150 mm, a total length of 600 mm, and an effective span of 450 mm. The net deflection was measured using two LVDTs installed at the mid-span section of the concrete beams, as shown in Fig. 7. The tests were displacement controlled to achieve a constant rate of net deflection at 0.1 mm/min. Three identical samples for each fibre type were tested. Two plain concrete beams were tested as the control specimens.

## 3. Results and discussion

The effects of PP and steel fibres on the flexural performance of concrete beams and ground slabs are not necessarily similar. Therefore, the flexural performance of notched beams, unnotched beams, and ground slabs are examined to evaluate the effectiveness of these two types of fibres on concrete beams vs ground slabs. Also, comparison between FRC ground slabs vs the one reinforced with steel meshes is made in this section.

### 3.1. Compressive strength

Fig. 8 shows the compressive strength of the fibre-reinforced concrete cubes. As can be seen, the compressive strength of PP fibre reinforced concrete was 45.7 MPa which showed a 4.3% increase as compared to that of plain concrete (43.8 MPa). It indicates the PP fibres had a marginal impact on the compressive strength of concrete. However, the steel fibre considerably improved the compressive strength to 47.5 MPa (8.4% improvement). This is because the PP fibres have lower elastic modulus (7 GPa) than concrete (22–38 GPa) and steel fibres (210 GPa) [27,28]. The experimental results agree well with the findings from the previous studies [29,30]. It is noted that both types of fibres

**Fig. 2.** Concrete slab casting.

**Fig. 3.** The compacted and low-plasticity sand in the sand containment box.

could reduce crack-tip stress concentration since fibres act as stress-transfer bridges, thus fibre-reinforced concrete showed ductile failure rather than brittle failure of plain concrete.

### 3.2. Post-cracking behaviour of fibre-reinforced concrete

Since the notched beam specimens are subjected to mid-point loading in the CMOD tests, a crack initiated at the notch-tip and propagated along the notch plane and hence, deformation was always localised at the notch-plane while the rest of the beam did not undergo significant inelastic deformation. This behaviour minimises the energy dissipated over the entire volume of the specimen and, therefore, all the energy absorbed can be directly attributed to fracture along the notch plane. Consequently, the energy dissipated in these tests can be directly correlated to material response (i.e. fibre reinforcements) [31].

Fig. 9 and Table 3 show the post-cracking behaviour of fibre-reinforced concrete, which can be characterised by the residual flexural strength of the notched concrete beams. The steel fibre and PP fibre-reinforced concrete showed a slightly higher flexural strength than that of plain concrete. With an increase in the CMOD, the applied loads of all the concrete beams reached the peak (around 16.5 kN), followed by a sudden drop at the CMOD of around 0.5 mm. The applied load of plain concrete decreased to nearly 0 kN at the $CMOD_1$, while the applied loads of PP fibre and steel fibre-reinforced concrete decreased to about 7.3 kN and 12.7 kN on average at the $CMOD_1$, respectively. The SFRC further decreased to 11.4 kN at the $CMOD_3$, while the PFRC increased to 8.7 kN at the $CMOD_3$. The energy absorption can be estimated as the areas of the Load-CMOD diagrams. The average energy absorptions of PP fibre and steel fibre-reinforced concrete were 33.0 J and 48.5 J, respectively, while the plain concrete was only 4.0 J, which demonstrated a significant improvement (8–12 times) in the energy absorption of FRC as compared to plain concrete. The energy absorption of SFRC was about 50% higher than that of PFRC.

### 3.3. Flexural performance of fibre-reinforced concrete

The flexural performance was also studied by using four-point loading tests on the unnotched beams, which characterises the flexural performance of the whole fibre-reinforced concrete beams. According to ASTM C1609 [32], the first peak strength, residual strength, toughness, and equivalent flexural strength ratio are calculated. Toughness was calculated by the total area under the load–deflection curve up to deflection of 1/150 (3 mm) of the span length. The equivalent flexural

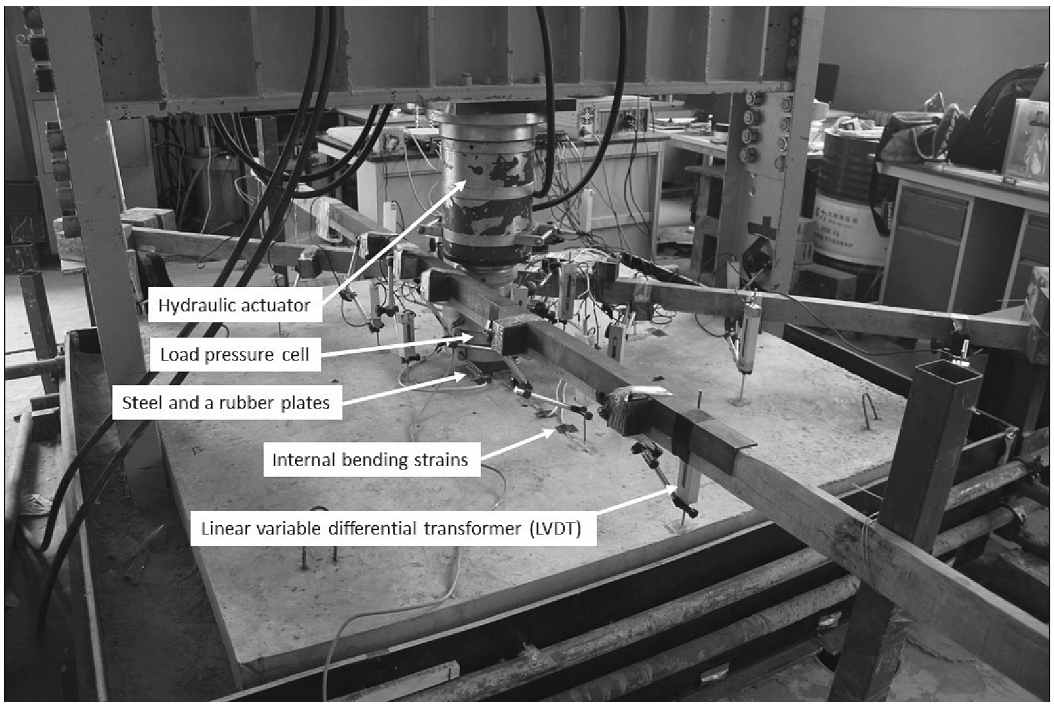


**Fig. 4.** The layout of the ground slab and test rigs.

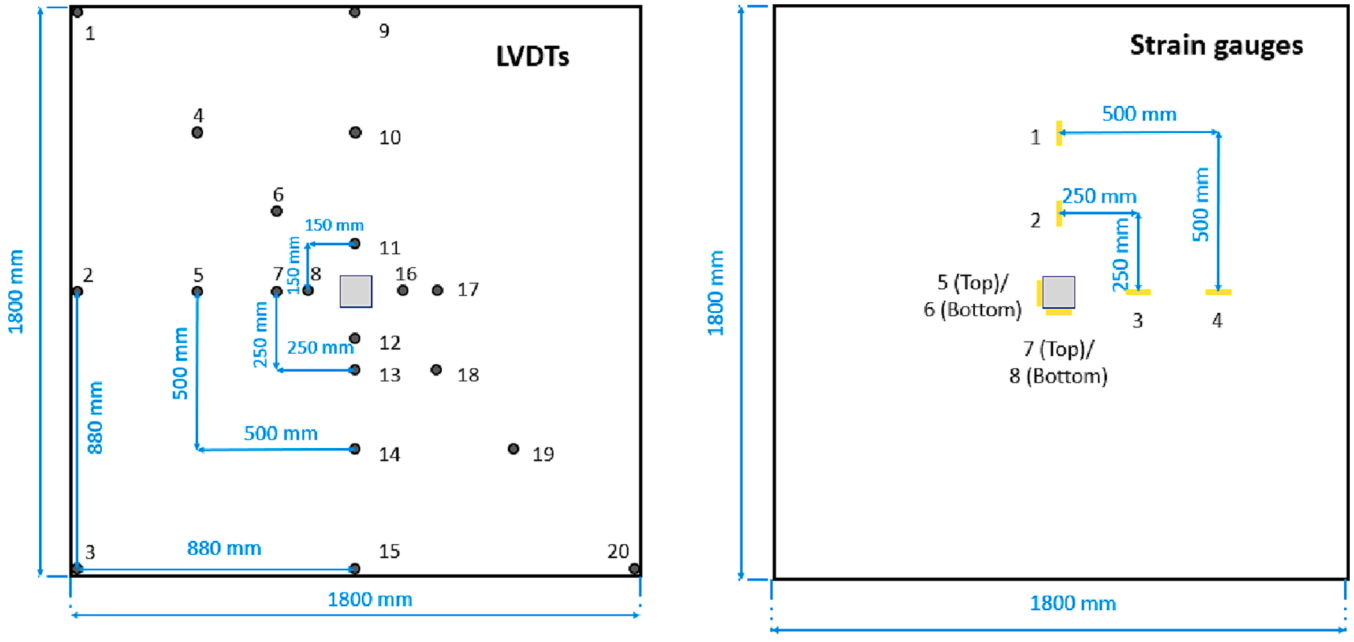


**Fig. 5.** Locations of the LVDTs and strain gauges on each slab.

strength ratio was calculated according to the flowing equation:

$$R_{e,3} = \frac{150 \times T_{150}^{D}}{f_1 \times b \times d^2} 100\% \quad (1)$$

where $R_{e,3}$ is the equivalent flexural strength ratio, $T_{150}^{D}$ is the toughness in J, $f_1$ is the first peak strength in MPa, and $b$ and $d$ are the width and depth of specimens in mm, respectively, which are both 150 mm.

As shown in Fig. 10, the SFRC beam had the highest first peak strength among all the concrete beams. The first peak strength was then followed by the second peak strength which was similar to or even higher than the first peak strength, showing deflection-hardening performance. The PFRC beam had a slightly lower first peak strength than that of steel fibre-reinforced beam, but the first peak strength was followed by a sudden drop, showing deflection-softening behaviour. It is interesting to note that PP fibre-reinforced beam showed comparable toughness with steel fibre-reinforced beam when the deflection increased to approximately 2–3 mm, as listed in Table 4. This phenomenon has shown that at large deformation, the performance of PFRC is as good as that of SFRC. Similar observations were also made in the previous studies [33,34].

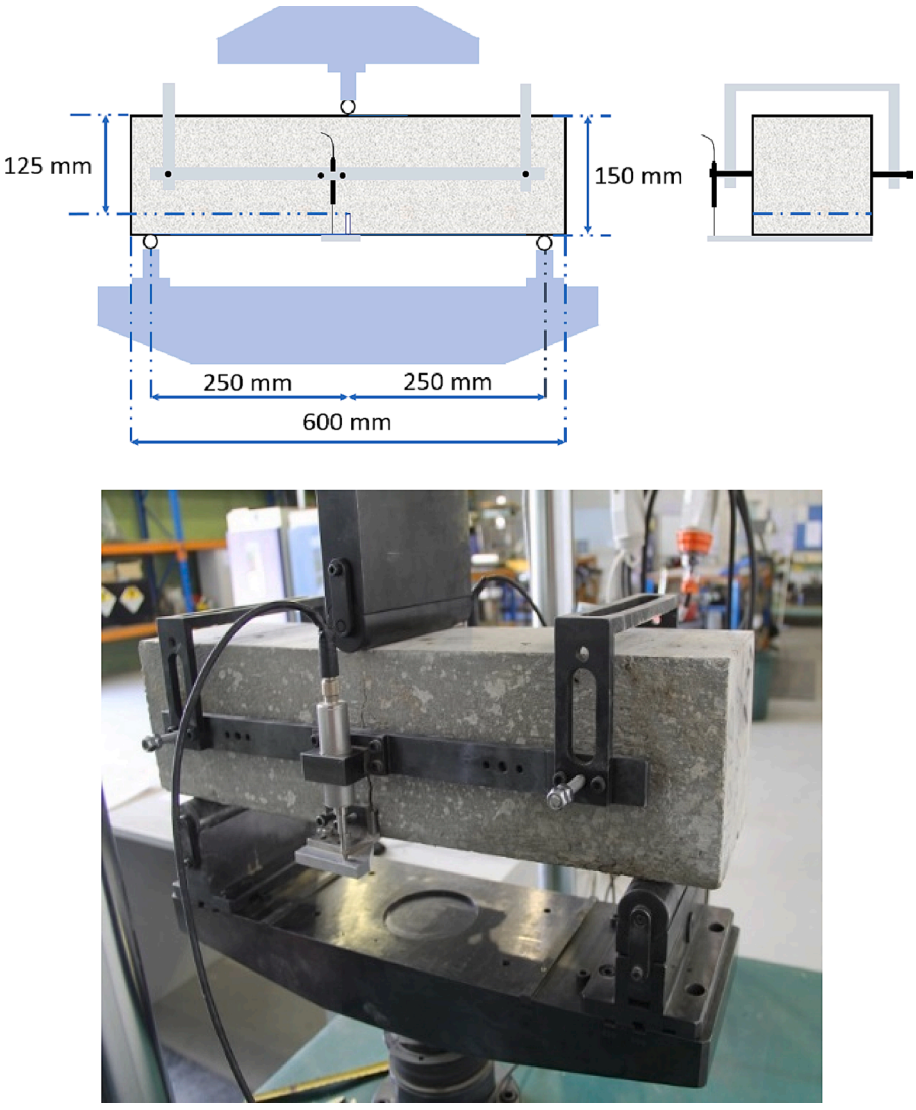


**Fig. 6.** Experimental setup for determining load-CMOD relationships.

### 3.4. Responses of ground slabs

#### 3.4.1. Applied load–strain responses

To examine the crack initiation and propagation, the strain gauges were attached close to the loading point. Two strain gauges (SG 5 and 7) were positioned on the top concrete surface for the compressive strain while the tensile strain gauges (SG 6 and 8) were attached to the bottom surface of the slab. In this study, cracks on the surface of slabs did not cross over SGs 1–4, so only the strains recorded at gauges (SG 5 to 8) will be discussed.

As shown in Fig. 11, the tensile strain gauges at the bottom of the plain concrete slab detected the initial micro cracks produced at the load of 25 kN, where the strain began to display nonlinear behaviour. When the applied load increased to 45 kN, there was another turning point, indicating that the micro cracks were expanding to macro cracks. For the PFRC slab, the macro cracks were observed at the applied load of 50 kN, and the applied load continued to increase with the tensile strain, indicating that fibres bridged the cracks and bore the applied load. It is interesting to note that only the load–strain curve of the plain concrete showed an obvious micro cracking point when initial micro cracks occurred, followed by the turning point when macro cracks formed. It is because without reinforcements stress was easy to concentrate on the loading point, forming micro cracks at a very low load. The steel fibre or steel mesh reinforcements can effectively mitigate the concentrated stress, thus no obvious turning point is shown when micro-cracks initiated and only macro cracks can be detected by the strain gauges.

The macro cracks of PP fibre-reinforced slab were observed at the applied load of 50 kN, which was slightly higher than that of plain concrete. The PP fibres had a lower elastic modulus (7 GPa) than that of concrete (20–30 GPa), thus the actions of PP fibres became prominent only after concrete experienced relatively large strain and deformation. Then fibres begun to reinforce after concrete cracking and the applied load of the PFRC slab continued to increase with the increase of strain after macro cracking point, while the applied load of plain slab remained approximately flat. This observation of ground slab response was consistent with the results of flexural tests of concrete beams in Fig. 9 and Fig. 10, where the PFRC beam had slightly higher flexural strength and first peak load than the plain concrete beam. On the other hand, the elastic modulus of steel fibres was 210 GPa, which was much higher than those of PP fibres and plain concrete, thus steel fibres began to significantly reinforce concrete at an early deformation stage. As a result, steel fibres reinforced concrete slab could bear a higher load (around 75 kN) before showing macro cracks. The applied load continued to increase with the increase of strain until macro cracking point due to the crack bridging effects of steel fibres.

Although the steel fibre-reinforced concrete slab could bear the

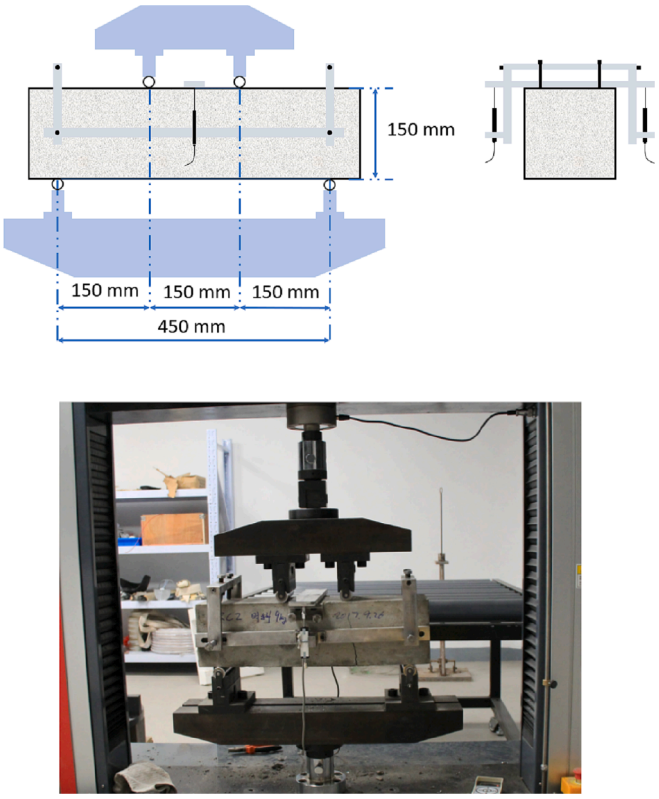


**Fig. 7.** Experimental setup for determining load–deflection relationships.

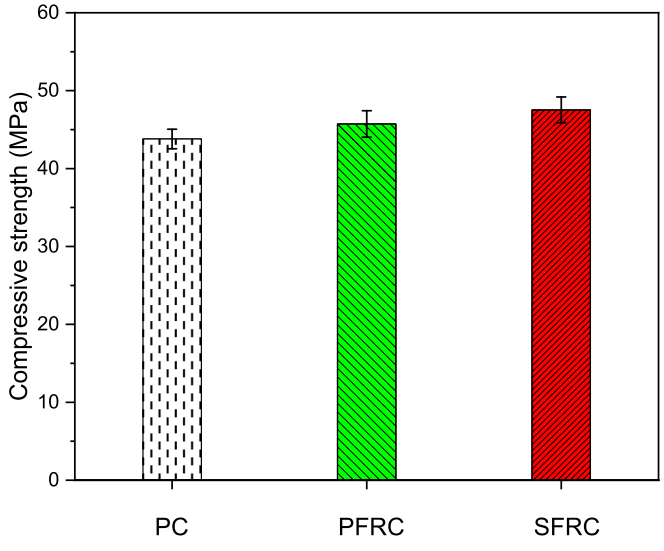


**Fig. 8.** Compressive strength of the plain concrete and fibre-reinforced concrete.

higher load than the slab reinforced with PP fibres, it is interesting to note that the slope of the SFRC after macro cracking load curve, corresponding to micro strain from 750 to 4000, was smaller than that of PFRC. It suggests that PP fibres were more resistant to uplift than steel fibers. The hardness of steel fibres is much higher than that of concrete. When steel fibres bridged cracks of concrete and interacted with concrete, the hard steel would break brittle concrete, leading to significantly decreased bonding between steel fibres and concrete. On the contrary, PP fibres are much softer than concrete. When PP fibres bridge concrete, soft PP fibres were deformed rather than concrete cracked. Because PP fibres were not brittle, the deformed PP fibres do not decrease the

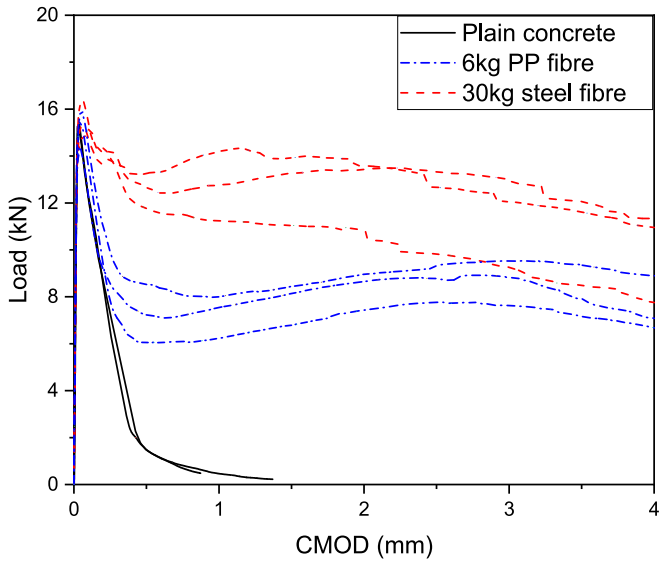


**Fig. 9.** Load-CMOD diagrams of fibre-reinforced concrete.

bonding between PP fibres and concrete, and even improve the bonding strength due to their deformed surfaces. Therefore, the PP fibres were more resistant to uplift than the steel fibers after the macro cracking point. This is an interesting observation, and it requires further studies to confirm.

The applied load of the SMRC slab reached 100 kN before the tensile strain significantly increased. The results showed that using steel mesh was the most effective reinforcing method for bearing the applied load. However, once the load reached 100 kN, the concrete cover under the steel mesh totally cracked. The applied load did not increase while the strain rose significantly, which was very different from the other three ground slabs as shown in Fig. 11.

All the slabs showed a similar increase trend in load-compressive strain responses before strain reached about 500 microstrain as shown in Fig. 11, indicating that fibre and mesh reinforcements had slight effects on the concrete compressive behaviour. When the compressive strain further increased to −3000, the rise (slope) of the applied load of the SMRC slab was highest followed by that of steel fibre-reinforced ground slab, indicating that the steel mesh and steel fibre-reinforced concrete slabs had higher stiffness than other slabs. The PFRC slab and plain concrete slab had lower load increase and even load reduction, showing their lower stiffness. This observation is reasonable due to the low modulus of PP fibres as mentioned previously.

### 3.4.2. *Applied load–deflection responses*

The applied load–deflection responses of the concrete slabs on the ground are shown in Fig. 12. The SMRC slab had the highest flexural cracking load (122 kN), while the steel fibre and PP fibre-reinforced concrete slabs had the flexural cracking load of 100 kN and 87 kN, respectively. For the specimens with fibre or steel mesh reinforcements, stress transferred to the fibres or steel meshes as concrete cracked, thus the slabs still kept resisting load and resulted in a high load-carrying capacity. The plain concrete slab had the lowest flexural cracking load of 68 kN, followed by a sudden reduction in the applied load to 40 kN. When the central deflection was over 6 mm, the plain concrete slab still resisted load. At this stage, the load was in fact mainly bore by the ground and the slab had mostly lost its load-carrying capacity. At 23.3 mm, the cracked plain concrete slab experienced punching shear failure at 95.9kN. It was different from the beam tests in Fig. 9 and Fig. 10, where fibre-reinforced concrete beams had slightly higher flexural strength and first peak strength than plain concrete, and the cracking load of PFRC ground slab was significantly higher than that of the plain concrete ground slab. It also could be found that SFRC beams performed

**Table 3**
Results of residual flexural strength of concrete.

| Sample | | Flexural strength(MPa) | Residual flexural strength (MPa) at | | | | Energy absorption(J) |
|---|---|---|---|---|---|---|---|
| | | | $CMOD_1$ | $CMOD_2$ | $CMOD_3$ | $CMOD_4$ | |
| Plain concrete | 1 | 4.91 | 0.15 | 0 | 0 | 0 | 4.20 |
| | 2 | 4.89 | 0 | 0 | 0 | 0 | 3.83 |
| 30 kg/m$^3$ Steel fibre | 1 | 4.89 | 4.54 | 4.36 | 3.86 | 3.51 | 52.18 |
| | 2 | 4.85 | 3.60 | 3.46 | 2.96 | 2.48 | 41.79 |
| | 3 | 5.24 | 4.09 | 4.30 | 4.16 | 3.63 | 51.66 |
| 6 kg/m$^3$ PP fibre | 1 | 4.61 | 2.42 | 2.77 | 2.82 | 2.27 | 33.23 |
| | 2 | 4.98 | 2.00 | 2.38 | 2.44 | 2.14 | 29.32 |
| | 3 | 5.12 | 2.56 | 2.87 | 3.05 | 2.85 | 36.46 |

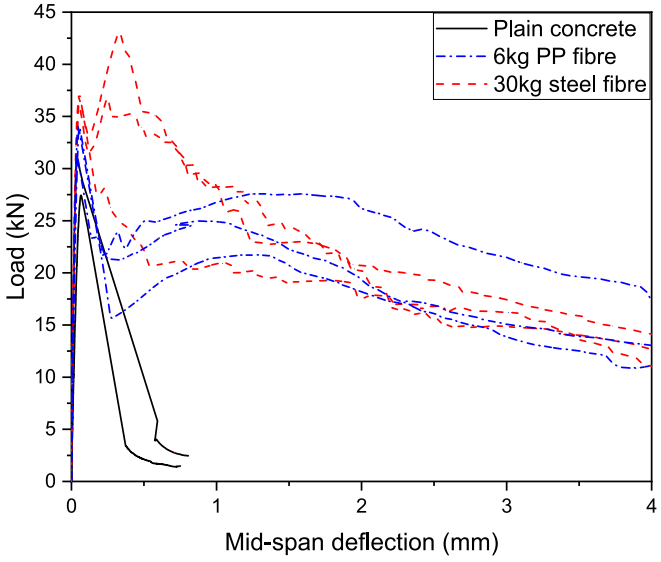


**Fig. 10.** Load-deflection diagrams of plain and fibre-reinforced concrete beams.

better than PFRC beams in both the residual flexural strength and flexural strength. However, when these two types of fibres were used to reinforce the ground slab, they had comparable reinforcing effects that the energy absorption of the SFRC slab was 2872 J and that of the PFRC slab was 2948 J. The applied load of the PFRC ground slab was even higher than that of the SFRC ground slab at deflection between 12.8 and 20 mm. At deflection of 20 mm, the applied load of PFRC and SFRC ground slabs was similar, about 120 kN.

### 3.4.3. Slab deflection profile and cracking levels

The surface deflection profiles at different levels of the ground slab central deflections are shown in Fig. 13. Deflection in the diagonal line of the slab was captured by LVDTs. When the central deflection increased from 0 to 5 mm, all the slabs maintained full contact with subgrade soil, which deformed almost uniformly with the slab. Since the plain concrete had already severely cracked at the deflection of 5 mm as shown in Fig. 12, when the central deflection increased to 10 mm, the edges and corners of the plain concrete slab and PFRC slab began to lose contact with the soil layer since they deflected upward. In Fig. 13, the steel fibre and steel mesh reinforced slabs still maintained nearly full contact with the soil at the central deflection of 10 mm, at which these slabs just began cracking as shown in Fig. 12. With further increase of the central deflection to 20 mm, an increase of non-contact area between the slab and supporting soil was observed in all the slabs due to higher level of deformations. When the central deflection reached 25 mm, the distance between the edge and center of plain concrete was 75 mm, while this distance of both the PP fibre and steel fibre-reinforced slabs was about 45 mm, which was slightly higher than that of the steel mesh reinforced slab (40 mm). In conclusion, similar to steel mesh reinforcement, the PP fibre and steel fibre reinforcement significantly decreased the deformation of the slabs subjecting to a central load.

Fig. 14 shows the crack patterns of all the slabs after testing. As can be seen, the plain concrete slab and fibre-reinforced concrete slabs failed with the initiation of four major cracks which started from the slab centre and developed along the median lines, while the steel mesh reinforced slab failed with five major cracks. The failure mode of the PFRC slab is similar to those in the previous study [22].

Fig. 15 shows the zoomed-in views of the patterns of cracks underneath the applied central load. During the tests, the plain concrete showed brittle instantaneous failure, followed by the sudden growth of cracks across the entire slab. Continuously applying load on plain concrete resulted in a shear failure in the centre of the slab. The maximum distance between the periphery of cracks and the centre point was 13 cm. The fibre and steel mesh reinforced slabs also showed circumferential cracks on top of the slab around the load plate. Meanwhile, the maximum distance between the periphery of cracks and the centre point of PP fibre and steel fibre-reinforced slabs were 13 cm and 27 cm, respectively, while the slab reinforced by steel meshes showed the largest distance of 40 cm. The diameter of circumferential cracks of the PFRC slab was slightly greater than that of the plain concrete slab while that for the SFRC slab was in between those of the PFRC and SMRC slabs. It can be found that with the reinforcement in concrete, the diameter of cracks became larger than plain concrete, and only plain concrete slab experienced clear punching shear failure.

**Table 4**
Results of the flexural strength of concrete beams.

| Sample | | First peak strength (MPa) | At the deflection of 3 mm | | |
|---|---|---|---|---|---|
| | | | Residual strength(MPa) | Toughness(J) | Equivalent flexural strength ratio ($R_{e,3}$) |
| Plain concrete | 1 | 3.66 | 0 | 6.724 | 8.2% |
| | 2 | 4.13 | 0 | 10.670 | 11.5% |
| 30 kg Steel fibre | 1 | 4.97 | 2.16 | 60.267 | 53.9% |
| | 2 | 4.92 | 1.98 | 73.310 | 66.2% |
| | 3 | 4.82 | 2.32 | 75.728 | 69.8% |
| 6 kg PP fibre | 1 | 4.17 | 1.85 | 62.145 | 66.1% |
| | 2 | 4.55 | 2.01 | 57.631 | 56.3% |
| | 3 | 4.52 | 2.86 | 76.263 | 74.9% |

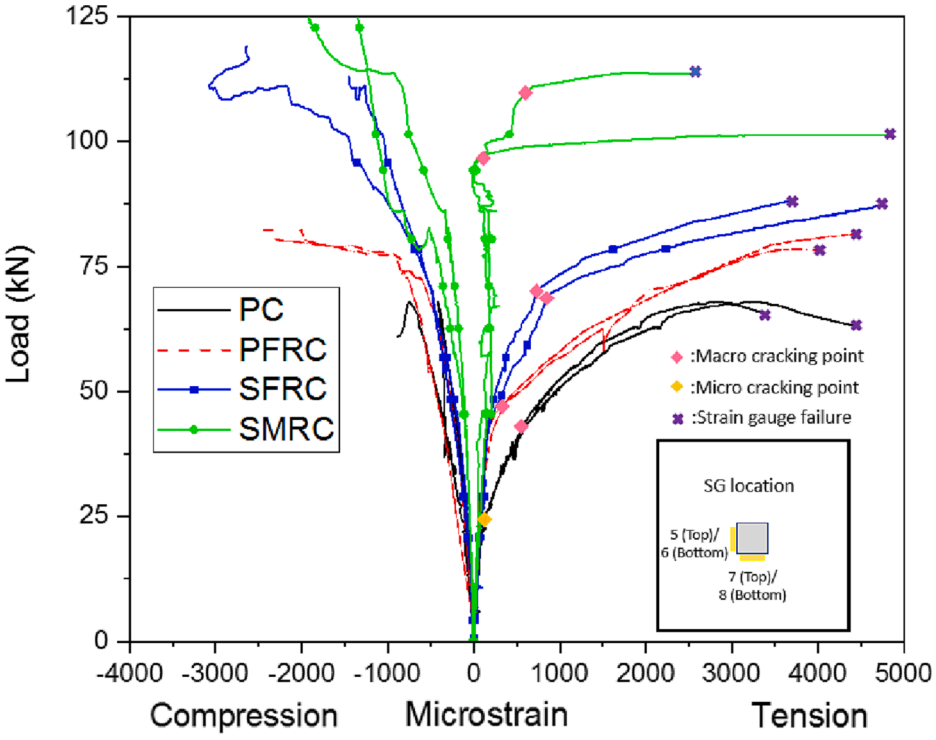


**Fig. 11.** Applied Load-strain responses of concrete slabs (SGs 5 to 8).

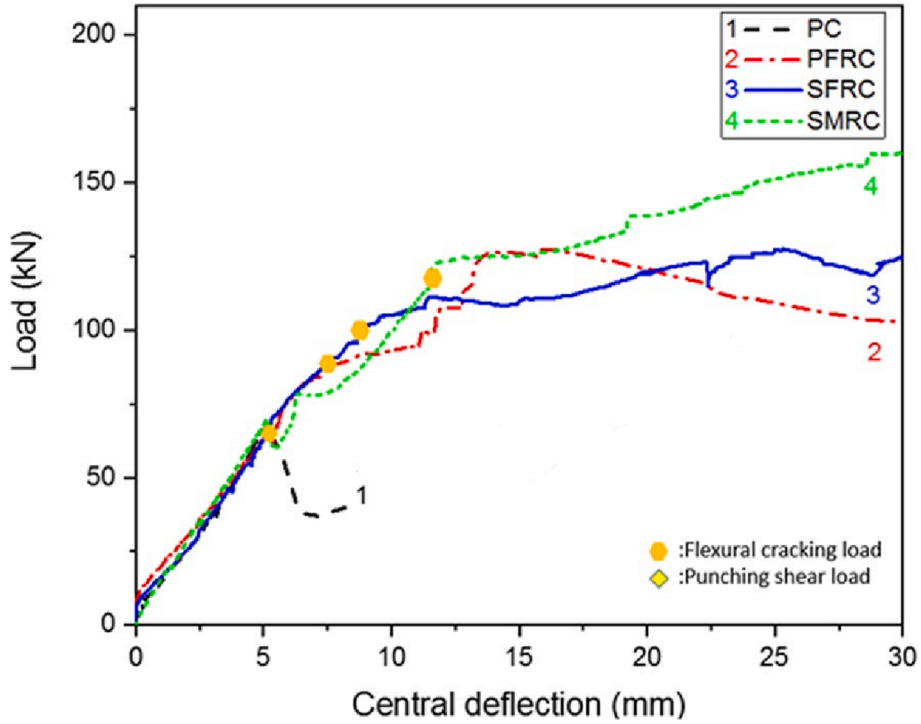


**Fig. 12.** Load-deflection responses of concrete slabs.

### 3.5. *Flexural and punching shear strength of the ground slab*

The flexural performance of FRC beams can be used to calculate the ultimate load-carrying capacity of the FRC ground slabs according to Technical Report 34 [35] based on the yield line theory. For an internal load, using the conventional yield line theory with true point load and ignoring the contribution of the subgrade reaction, the collapse load per unit length, $P_u$ could be calculated by the following equation:

$$P_u = 2\pi \times \left(M_p + M_n\right) \tag{2}$$

where $P_u$ is the collapse load capacity in kN.m/m, $M_p$ is the ultimate positive resistance moment per unit length of the slab in kN.m/m, $M_n$ is the ultimate negative resistance moment per unit length of the slab in

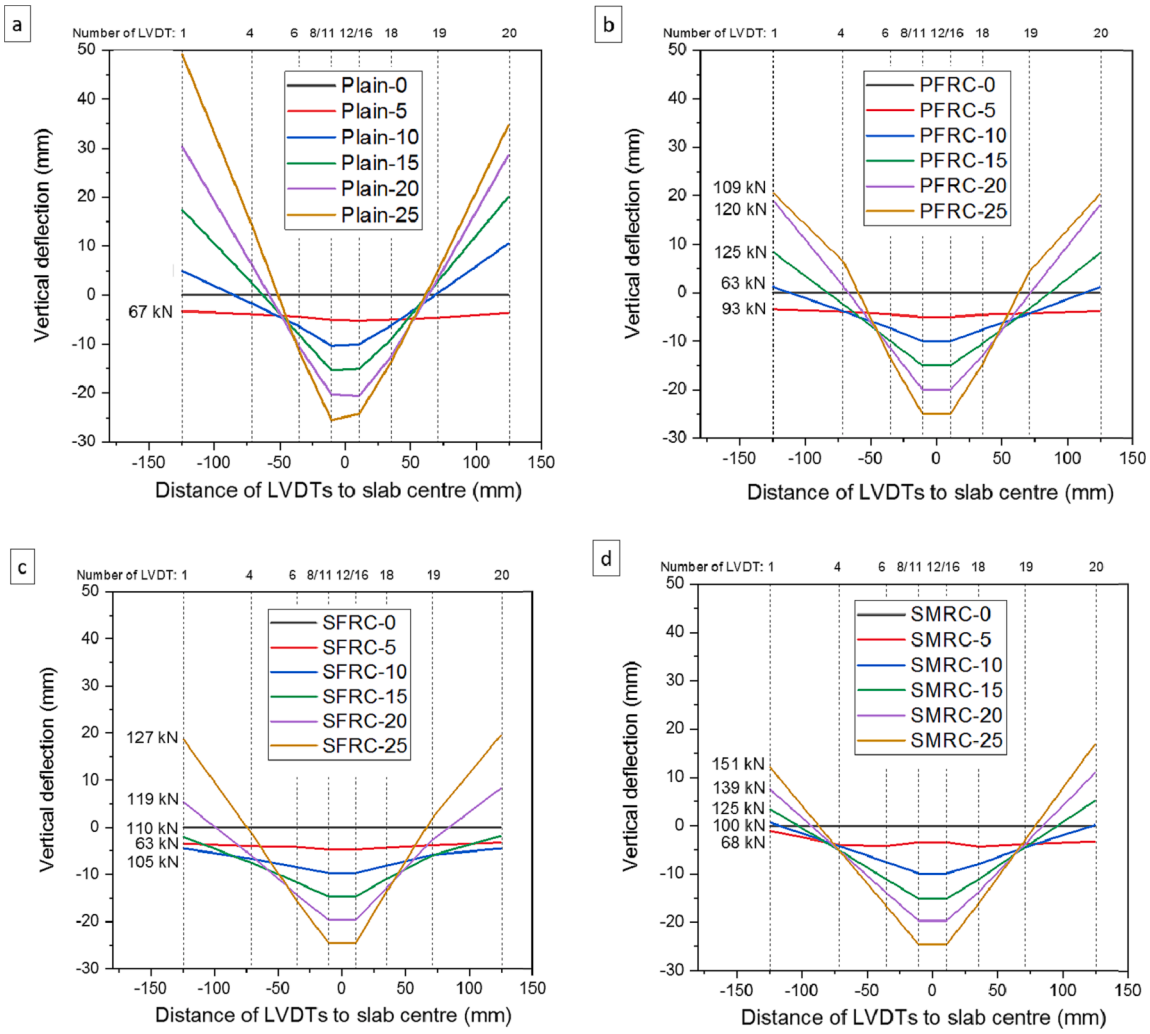


**Fig. 13.** Surface deflection profile at the levels of central deflection of 0, 5, 10, 15, 20 and 25 mm: (a) Plain concrete slab, (b) PP fibre-reinforced slab, (c) Steel fibre-reinforced slab, (d) steel mesh reinforced slab.

kN.m/m.

The equivalent flexural strength ratio, $R_{e,3}$, as a characterization of the ductility of fibre-reinforced concrete is used to calculate the residual positive bending moment capacity per unit length, $M_{p,fibre}$ as follows:

$$M_{p,fibre} = \frac{f_{ctk,fl}}{\gamma_c} \times (R_{e,3}) \times (\frac{h^2}{6}) \quad (3)$$

where $f_{ctk,fl}$ is the characteristic flexural strength of plain concrete in MPa, $\gamma_c$ is the partial safety factor for concrete and $h$ is the slab thickness in mm.

The negative bending moment capacity per unit length, $M_n$ is assumed that cracking stress is not influenced by the increase of ductility due to fibre. The following equation is used to calculate $M_n$ as follows:

$$M_n = \frac{f_{ctk,fl}}{\gamma_c} \times (\frac{h^2}{6}) \quad (4)$$

For steel mesh reinforcement, the negative bending moment capacity per unit length is the same as Equation 4 and the positive bending moment capacity per unit length is calculated by the following equation:

$$M_{p,SM} = \frac{0.95A_s \times f_y \times d}{\gamma_s} \quad (5)$$

where $A_s$ is the area of steel mesh in mm$^2$, $f_y$ is the characteristic strength of steel in MPa, $d$ is the effective depth in mm and $\gamma_c$ is the partial safety factor for steel.

Table 5 summarises the test results of the beams and slabs and the calculated results based on TR34 [35]. It can be seen that the improvements in the flexural strengths of plain and FRC from four-point beam flexural tests were minor (1.13 and 1.26 times for PFRC and SFRC larger than plain concrete) as compared to those obtained in the tests of ground slabs in this study. The corresponding values were 1.28 and 1.47 times for PFRC and SFRC. Comparing the normalized collapse load of slabs (fibres, mesh/plain) with the calculated normalized collapse load (fibres, mesh/plain), it could be seen that the method from TR34 [35] could be used to estimate the collapse load of ground slabs with steel mesh or SFRC with reasonable accuracy. However, the calculated collapse loads based on TR34 [35] were higher than the actual test results of slabs on the ground. The calculated/experimental collapse load ratio of plain concrete and SMRC is the same, at 1.12, while that of PFRC and SFRC is higher at 1.45 and 1.24, respectively. This indicated that this method would overestimate the cracking load of slab on the ground reinforced by fibres, especially PP fibres, because this method is relied on $R_{e,3}$ (equivalent flexural strength ratio) from the post-cracking performance of FRC beams to predict the cracking load of slabs on the ground. It means the contribution of the post-cracking performance of FRC to the ground slab is not accurately estimated. Given the same beam size with different types of fibres, as long as the two beams have the same ratio of $T^D_{150}$ and $f_1$, they would have the same equivalent flexural strength ratio ($R_{e,3}$) but the peak strength $f_1$ can be

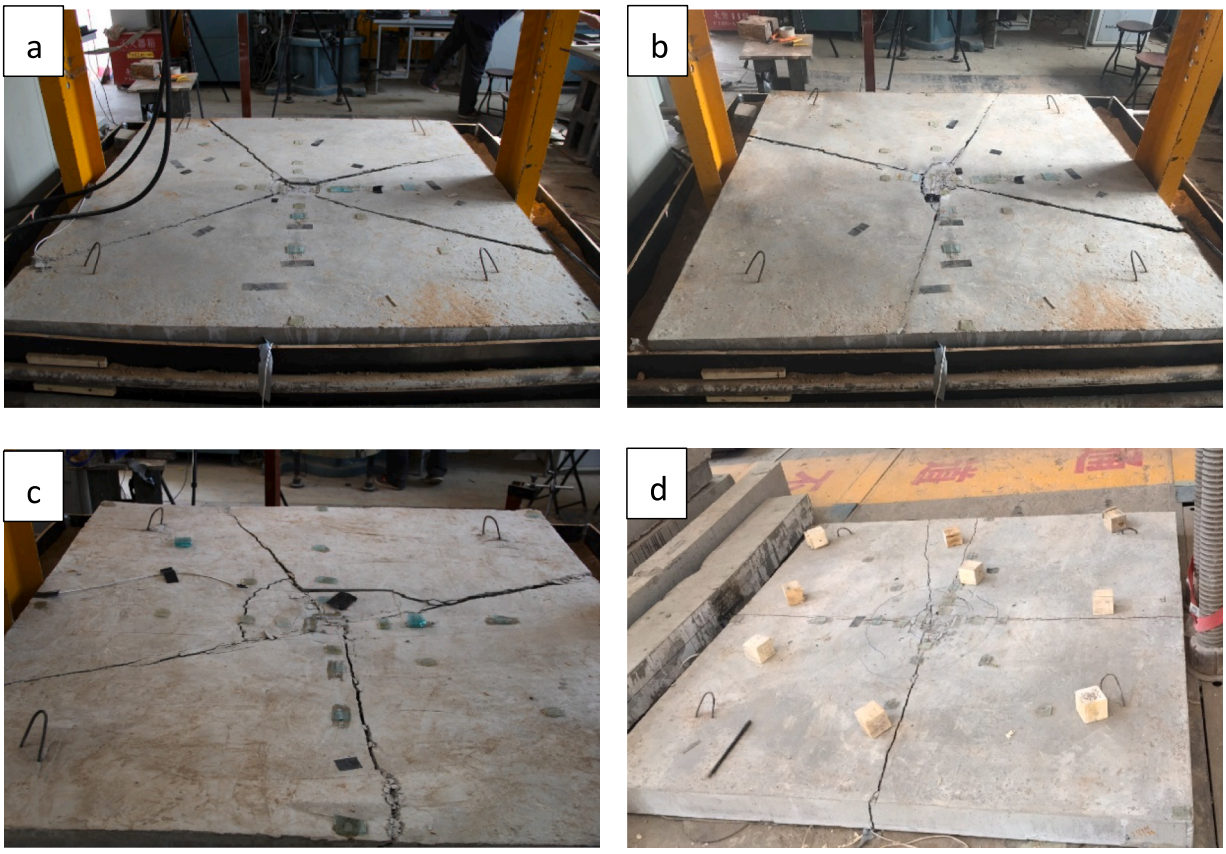


**Fig. 14.** Crack patterns in the slabs: (a) plain concrete; (b) PFRC; (c) SFRC; (d) SMRC.

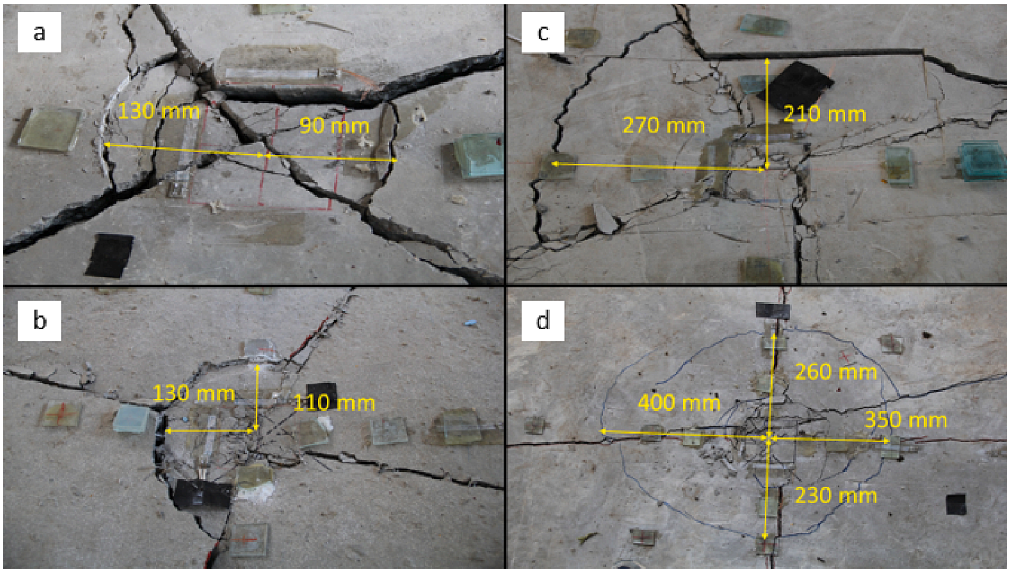


**Fig. 15.** Distance between the periphery of cracks and centre point on the top surface of concrete slab: (a) plain concrete, (b) PFRC, (c) SFRC, and (d) SMRC.

very different. Accordingly, the calculated collapse load from TR34 [35] method would be similar. Therefore, this design procedure cannot accurately predict the performance of FRC slabs reinforced with different fibres. A new design procedure is deemed sought for a more accurate prediction in which the peak flexural strength of FRC should be considered.

In addition, the punching shear capacity of slabs is also an important property during the slab design. In this study, the estimated punching shear load as per TR34 [35] was used to compare with the test results. According to TR34 [35], the shear stress at the face of the contact area should be lower than a value $V_{\max}$ as follows:

$$V_{max} = 0.5 \times k_2 \times f_{cd} \tag{6}$$

where $f_{cd}$ is the compressive strength of concrete cylinders in MPa.

Therefore, the maximum punching load capacity, $P_{p,\max}$ can be calculated as follows:

**Table 5**
Summary of test result and calculated cracking load and shear load.

| Note | Note | Plain concrete | 6 kg/m$^3$ PP fibre | 30 kg/m$^3$ Steel fibre | Steel mesh |
|---|---|---|---|---|---|
| Notched beam flexural strength (MPa) | 1 | 4.90 | 4.90 | 5.00 | – |
| Normalized against plain concrete | 2 | 1.00 | 1.00 | 1.02 | – |
| Four-point bending peak strength (MPa) | 3 | 3.90 | 4.41 | 4.90 | – |
| Normalized against plain concrete | 4 | 1.00 | 1.13 | 1.26 | – |
| Calculated collapse load (kN) for 1.8x1.8 m slabs | 5 | 76.0 | 126.0 | 124.2 | 136.3 |
| Experimental collapse load of slab (kN) for 1.8x1.8 m slabs | 6 | 68 | 87 | 100 | 122 |
| Normalized against plain concrete | 7 | 1.00 | 1.28 | 1.47 | 1.79 |
| Calculated/tested flexural cracking | (5)/(6) | 1.12 | 1.45 | 1.24 | 1.12 |
| Calculated shear strength on critical perimeter | 8 | 96.16 | 96.16 | 123.55 | 200.29 |
| Normalized against plain concrete | 9 | 1.00 | 1.00 | 1.28 | 1.62 |

$$P_{p,max} = V_{max} \times u_0 \times h_{ed} \tag{7}$$

where $u_0$ is the length of the perimeter at the face of the loaded area, $h_{ed}$ is the effective depth, taken as 0.75 $h$ for plain concrete and FRC.

For plain concrete slabs, the minimum shear strength should be taken as:

$$V_{Rd,c} = 0.035 \times k_1^{\frac{3}{2}} \times f_{ck}^{\frac{1}{2}} \tag{8}$$

$$k_1 = 1 + (200/h_{ed})^{0.5} \leqslant 2 \tag{9}$$

Thus, the plain slab shear capacity, $P_p$, can be calculated as follows:

$$P_p = V_{Rd,c,plain} \times u_1 \times h_{ed} \tag{10}$$

where $u_1$ is the length of the perimeter at a distance of twice of the effective depth $h_{ed}$ from the loaded area.

For SFRC slabs, the increased shear capacity from steel fibres $V_f$ over that of plain concrete based on TR34 guidance [35] can be calculated as:

$$V_f = 0.12 \times f_{ctk,fl} \times R_{e,3} \tag{11}$$

Combined with the minimum shear strength $V_{Rd,\ c}$, the SFRC slab shear capacity is given by:

$$P_{SF} = (V_{Rd,c,plain} + V_f) \times u_1 \times h_{ed} \tag{12}$$

For SMRC slabs, the average shear stress can be calculated by:

$$V_{Rd,c} = \frac{0.18}{\gamma_c} \times k_1 \times (100 \times \rho_1 \times f_{ck})^{\frac{1}{3}} \geq 0.035 \times k_1^{\frac{3}{2}} \times f_{ck}^{\frac{1}{2}} \tag{13}$$

where $\rho_1 = (\rho_x \times \rho_y)^{\frac{1}{2}}$, $\rho_x and \rho_y$ are the reinforcement ratios by area in the x- and y-direction, respectively.

For PFRC slabs, there is no guidance available currently to calculate shear capacity. Obviously, using the same formula from TR34 [35] is not suitable due to macro PP fibres cannot provide a similar reinforcing effect on shear strength as steel fibres. Therefore, it should be assumed that the shear capacity is that of plain concrete as suggested by TR34 [35].

As shown in Fig. 12, the applied load of slabs was all lower than the predicted punching shear capacity of 201 kN, implying the tested slabs met the requirement of punching load capacity, but failed due to flexural bending as observed above. Punching shear is a result of a concentrated load on a relatively small area around the loaded area and a control area on the top and bottom of the slab, respectively. Therefore, the shear stress is checked on the critical shear perimeter at a distance $2h_{ed}$ (effective depth of slab) from the loaded area.

In brief, the estimated shear strength on the critical perimeter was listed in Table 5. It can be seen that the shear strength of the plain slab from the test (95.9 kN) matched well with the calculated shear strength (96.2 kN) while other slabs did not show a pure punching shear failure.

## 4. Conclusions

This study performed experimental tests of concrete ground slabs with different reinforcing types, including plain, steel meshes, steel fibres and macro PP fibres. Four different slabs on the ground were subjected to concentrated loading at the centre of the slab. The influences of different fibre reinforcements on the performance of concrete ground slabs were discussed. The following conclusions can be drawn.

1. The experimental results have shown that the structural performance of the PFRC ground slab was much better than the plain concrete slab and comparable to the SFRC ground slab. However, the PP fibre reinforcement did not effectively mitigate the flexural crack as steel fibre reinforcement of ground slabs.
2. The addition of 30 kg/m$^3$ steel fibres and 6 kg/m$^3$ PP fibres increased the flexural cracking load by 47% and 28% compared to the plain concrete slab, respectively, while the slab with A142 steel meshes had the highest load capacity, i.e., 79% higher than the plain concrete slab. The use of 6 kg/m$^3$ PP fibres compared favorably with 30 kg/m$^3$ steel fibres in terms of post-cracking performance and energy absorption of ground slabs.
3. The use of PP fibres had little influence on the distance between the periphery of cracks and centre point on top surface while steel fibres and steel meshes could increase that distance by 220% and 280%, respectively. In terms of deformation resistance, steel fibres and PP fibres could significantly improve ability of deformation resistance of slabs under central load compared with the plain concrete slab. Using steel meshes was the most effective to control slab deformation.
4. Adding 30 kg/m$^3$ steel fibres and 6 kg/m$^3$ PP fibres could improve the flexural strength of concrete beams by 13% and 26%, and ground slab by 28% and 47%.
5. The collapse loads predicted based on the beam flexural test and steel mesh properties were larger than the experimental flexural strength of the tested ground slabs. Overestimations of the flexural strength for plain concrete and SMRC ground slab are approximately 10%, while those for PFRC and SFRC are 45% and 24%, respectively.
6. The predictive method from TR34 [35] overestimates the flexural cracking loads of fibre-reinforced ground slabs.

## CRediT authorship contribution statement

**Feng Shi:** Data curation, Investigation, Methodology, Writing – original draft. **Thong M. Pham:** Conceptualization, Supervision, Writing – review & editing. **Rabin Tuladhar:** Writing – review & editing. **Zongcai Deng:** Resources, Writing – review & editing. **Shi Yin:** Methodology, Writing – review & editing. **Hong Hao:** Funding acquisition, Writing – review & editing, Supervision.

## Declaration of Competing Interest

The authors declare that they have no known competing financial interests or personal relationships that could have appeared to influence the work reported in this paper.

## Acknowledgement

The financial support from the Australian Research Council (Australia) Laureate Fellowships FL 180100196 is acknowledged.

## References

[1] Zheng Y, Zhou LZ, Taylor SE, Ma HW. Serviceability of one-way high-volume fly ash-self-compacting concrete slabs reinforced with basalt FRP bars. Constr Build Mater 2019;217:108–27.
[2] Awad R, Barakat S, Leblouba M, Altoubat S, Maalej M. Reliability-based design of fiber reinforced concrete slabs-on-ground in flexure as per ACI 360. Structures 2022;39:207–17.
[3] Soares D, de Brito J, Ferreira J, Pacheco J. Use of coarse recycled aggregates from precast concrete rejects: mechanical and durability performance. Constr Build Mater 2014;71:263–72.
[4] Boyer L. Decorative concrete has come a long way! Concr Int 2002;24(6):62–7.
[5] Alani AM, Beckett D. Mechanical properties of a large scale synthetic fibre reinforced concrete ground slab. Constr Build Mater 2013;41:335–44.
[6] Yin S, Tuladhar R, Shi F, Combe M, Collister T, Sivakugan N. Use of macro plastic fibres in concrete: a review. Constr Build Mater 2015;93(15):180–8.
[7] El-Sayed TA. Flexural behavior of RC beams containing recycled industrial wastes as steel fibers. Constr Build Mater 2019;212:27–38.
[8] Yousefi M, Khandestani R, Gharaei-Moghaddam N. Flexural behavior of reinforced concrete beams made of normal and polypropylene fiber-reinforced concrete containing date palm leaf ash. Structures 2022;37:1053–68.
[9] Amiri M, Reza EM. Effect of using Engineered Cementitious Composites (ECC) on failure behavior of flat slab-column connections. Structures 2023;47:2397–407.
[10] Hao YF, Hao H. Pull-out behaviour of spiral-shaped steel fibres from normal-strength concrete matrix. Constr Build Mater 2017;139:34–44.
[11] Yin S, Tuladhar R, Riella J, Chung D, Collister T, Combe M, et al. Comparative evaluation of virgin and recycled polypropylene fibre reinforced concrete. Constr Build Mater 2016;114:134–41.
[12] Orouji M, Zahrai SM, Najaf E. Effect of glass powder & polypropylene fibers on compressive and flexural strengths, toughness and ductility of concrete: an environmental approach. Structures 2021;33:4616–28.
[13] Yin S, Tuladhar R, Combe M, Collister T, Jacob M, Shanks R. Mechanical properties of recycled plastic fibres for reinforcing concrete. In: Proceedings of the 7th International Conference Fibre Concrete, pp 1-10 From: 7th International Conference Fibre Concrete, September 12-13 2013, Prague, Czech Republic2013.
[14] Uğur AE, Ünal A. Assessing the structural behavior of reinforced concrete beams produced with macro synthetic fiber reinforced self-compacting concrete. Structures 2022;38:1226–43.
[15] Yin S, Tuladhar R, Collister T, Combe M, Sivakugan N, Deng ZC. Post-cracking performance of recycled polypropylene fibre in concrete. Constr Build Mater 2015;101(13):1069–77.
[16] Yin S, Tuladhar R, Collister T, Combe M, Sivakugan N. Mechanical Properties and Post-crack Behaviours of Recycled PP Fibre Reinforced Concrete. In: Proceedings of the 27th Biennial National Conference of the Concrete Institute of Australia, Construction Innovations, Research into Practice, pp 414-421 From: 27th International Conference Concrete 2015, 30 August-2 September, 2015, Melbourne, Australia. 2015.
[17] Yin S, Tuladhar R, Shanks RA, Collister T, Combe M, Jacob M, et al. Fiber preparation and mechanical properties of recycled polypropylene for reinforcing concrete. J Appl Polym Sci 2015;132(16):n/a–.
[18] Deng ZC, Shi F, Yin S, Tuladhar R. Characterisation of macro polyolefin fibre reinforcement in concrete through round determinate panel test. Constr Build Mater 2016;121:229–35.
[19] Øverli J. Experimental and numerical investigation of slabs on ground subjected to concentrated loads. Central European Journal of Engineering 2014;4(3):210–25.
[20] Alani A, Beckett D, Khosrowshahi F. Mechanical behaviour of a steel fibre reinforced concrete ground slab. Mag Concr Res 2012;64(7):593–604.
[21] Roesler JR, Altoubat SA, Lange DA, Rieder KA, Ulreich GR. Effect of synthetic fibers on structural behavior of concrete slabs-on-ground. ACI Mater J 2006;103(1):3–10.
[22] Roesler JR, Lange DA, Altoubat SA, Rieder KA, Ulreich GR. Fracture of plain and fiber-reinforced concrete slabs under monotonic loading. J Mater Civ Eng 2004;16(5):452–60.
[23] As.. AS 1012.3.1: 2014 Methods of testing concrete Determination of properties related to the consistency of concrete - Slump test. Standards Australia; 2014.
[24] As.. AS 1012.8.1: 2014 Methods of testing concrete - Method for making and curing concrete - Compression and indirect tensile test specimens. Standards Australia; 2014.
[25] committee Cs. Standard for test method of mechanical properties on ordinary concrete (2003) (in Chinese). National standard of the People's Republic of China. 2002.
[26] EN B. BS EN 14651:2005+A1:2007 Test method for metallic fibre concrete. Measuring the flexural tensile strength (limit of proportionality (LOP), residual). 2005.
[27] Sharma M, Bishnoi S. Influence of properties of interfacial transition zone on elastic modulus of concrete: evidence from micromechanical modelling. Constr Build Mater 2020;246:118381.
[28] Shi F, Yin S, Pham TM, Tuladhar R, Hao H. Pullout and flexural performance of silane groups and hydrophilic groups grafted polypropylene fibre reinforced UHPC. Constr Build Mater 2021;277:122335.
[29] Dawood ET, Ramli M. High strength characteristics of cement mortar reinforced with hybrid fibres. Constr Build Mater 2011;25(5):2240–7.
[30] Shi F, Pham TM, Hao H, Hao Y. Post-cracking behaviour of basalt and macro polypropylene hybrid fibre reinforced concrete with different compressive strengths. Constr Build Mater 2020;262:120108.
[31] Jamet D, Gettu R, Gopalaratnam VS, Aguado A. Toughness of fiber-reinforced high-strength concrete from notched beam tests. Amer Conc 1995;I(155):23–39.
[32] Astm c1609.. Flexural Performance of Fiber-Reinforced Concrete (Using Beam With Third-Point Loading). ASTM C1609/C1609M-12. West Conshohocken, PA: ASTM International; 2012.
[33] Soutsos M, Le T, Lampropoulos A. Flexural performance of fibre reinforced concrete made with steel and synthetic fibres. Constr Build Mater 2012;36:704–10.
[34] Buratti N, Mazzotti C, Savoia M. Post-cracking behaviour of steel and macro-synthetic fibre-reinforced concretes. Construction and Building Material 2011;25(5):2713–22.
[35] Society C. Concrete industrial ground floors: a guide to design and construction. Concrete Society; 2003.